

Targeting Clause Type Distributions: a Picklock for Random Satisfiability Problems

Joachim Schwardt^{1,2*} and Jan Carl Budich^{1,2}

¹*Max Planck Institute for the Physics of Complex Systems,
Nöthnitzer Str. 38, 01187 Dresden, Germany and*

²*Institute of Theoretical Physics, Technische Universität Dresden and
Würzburg-Dresden Cluster of Excellence ct.d.qmat, 01062 Dresden, Germany*

(Dated: May 21, 2026)

Optimization problems such as the NP-complete 3-SAT provide an important benchmark for the difficult task of finding ground-states in strongly correlated many-body systems with rugged energy landscapes. The study of random 3-SAT problems as Ising spin Hamiltonians in statistical physics has yielded major insights including the existence of a satisfiability phase transition, and the prediction of a critical parameter line of particularly hard instances. Yet, progress on solving those instances has been scarce for several decades. Here, introducing the TARGET-SAT (TSAT) algorithm, we roughly triple the tractable problem sizes in the hardest regime, with an even greater improvement in a vast range of neighboring regions. By leveraging statistical information hidden in the combinatorial constraints of the problem, TSAT is actively guided in its stochastic local search toward a target within the relevant parameter space. Our analysis also explains why established local search algorithms are limited to relatively small system sizes due to a vast low-energy trap. Furthermore, we characterize the aforementioned critical line in terms of a dominant additional complexity barrier, whose exponential scaling is quickly overcome by TSAT only in the surrounding parameter space. With TSAT, the lead in solving the hardest known random satisfiability problems returns to the realm of stochastic local search algorithms.

I. INTRODUCTION

Finding the ground-state of a strongly correlated many-body system is among the foundational challenges in physics, which may be seen as a hard optimization problem arising from the emergence of local minima and barriers in rugged energy landscapes. Physically, such obstacles may for example be rooted in frustrated magnetic interactions, that amount to competing combinatorial constraints from a mathematical perspective. Owing to this close correspondence, mappings between Ising spin models in physics and abstract satisfiability problems [1, 2] have stimulated an active frontier of interdisciplinary research for decades, encompassing statistical physics [3–8], computational complexity theory [9–13], and constrained optimization [14–28]. In this context, the paradigmatic NP-complete 3-SAT problem has become a ubiquitous benchmark problem around which crucial progress has evolved in various directions.

For the generic case of random 3-SAT instances, there exists a sharp phase transition to non-zero ground-state energies (i.e. unsatisfiable problems) at a critical density α_c [12, 29–31] of combinatorial constraints. An important result from statistical physics is the explanation of this transition via the so-called cavity method at “one-step replica symmetry breaking level” [32, 33], which, although some mathematical concerns about its rigor remain [34–36], matches the numerical observations quite well. This approach has also shed light on the structure of the low-energy states, and thereby lead to the powerful SURVEY PROPAGATION (SP) algorithm [37, 38] capable

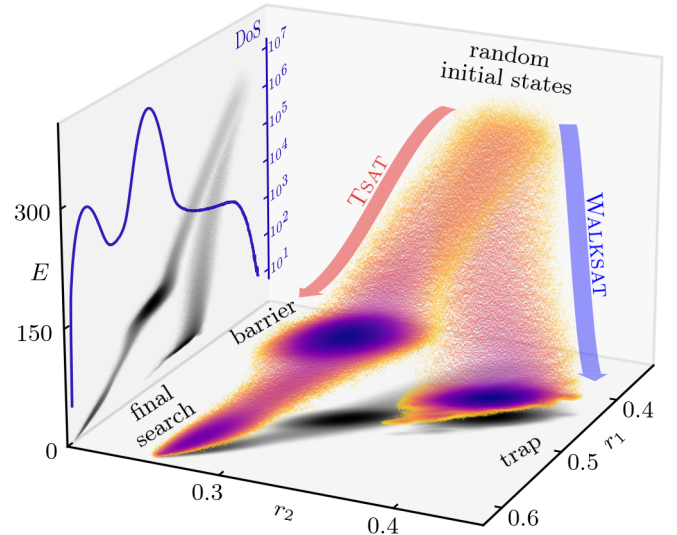


FIG. 1. Illustration of TSAT and WALKSAT trajectories through clause-type distribution space (CTDS), starting from random initial states. The color corresponds to the \log_{10} of the density of states (DoS), and for the TSAT trajectories we also show the accumulated DoS on the left (cf. Fig. 4). The grayscale projections are along the E and r_2 axes and serve as a visual guide. WALKSAT does not reach the solution at $E = 0$ because it gets stuck in a vast local minimum of low-energy states (trap). The TSAT algorithm introduced in this article takes a completely different path and encounters a barrier before entering a final search for the solution located near the bottom left.

of finding ground-states for very large systems close to the phase transition. However, further insights in the physical context of magnetism have revealed a parame-

* jschwardt@pks.mpg.de

ter regime for random 3-SAT problems that are beyond the capabilities of SP, and that always have zero-energy ground-states due to an inbuilt symmetry [39]. In particular, on a *critical line* [40] in the statistical distribution of problem parameters, ground-states have an extensive number of frozen spins (referred to as a *backbone*), whose magnetization is fixed across all ground-states thus allowing them to hide well in the exponentially large configuration space [39]. For such problems, all known optimization methods, including stochastic local search (SLS) [41–44], and so-called complete solvers [45–47], despite their remarkable advances on structured (practical) problems [48–50], are limited to modest problem sizes ($N \sim 500$), and have seen little progress over several decades.

Here, we present a SLS solver coined TARGET-SAT (TSAT) that roughly triples the tractable problem sizes to $N \sim 1500$ in the aforementioned hardest regime of 3-SAT, and that yields even greater improvement in an extended adjacent parameter region (cf. Fig. 3). Our findings are based on analyzing and harnessing the statistical properties of combinatorial constraints in random 3-SAT instances, organized in a phase space coined clause-type distribution space (CTDS) (cf. Fig. 1). Specifically, drawing inspiration from our recent more specialized heuristic DOCSAT [51], we generally discuss how the position in CTDS affects the difficulty of a problem, and how targeting this position provides efficient guidance to SLS beyond energy E as the primary figure of merit. This approach not only allows us to empirically confirm the predicted [39] critical line as the location of the hardest problems (cf. Fig. 2), but also to reveal a deeper structure of their complexity in terms of two separate barriers (cf. Fig. 1). Quite remarkably, with our TSAT algorithm the first complexity barrier representing the main bottleneck on the critical line (cf. Fig. 4) quite quickly becomes sub-exponential when moving away in CTDS (cf. Fig. 5). By contrast, the second complexity barrier dubbed *final search* generically remains exponential so as to reflect the NP-completeness of 3-SAT, and behaves smoothly around the critical line (cf. Fig. 6). Moreover, our study clarifies why well established SLS algorithms such as WALKSAT [41] inevitably run into a trap of local minima (cf. Fig. 1) as they do not deliberately target specific regions in CTDS. Outperforming all other methods in a wide parameter range including the hardest solvable 3-SAT problems, TSAT drastically advances and reclaims for SLS algorithms the forefront of solving random satisfiability problems.

II. CLAUSE-TYPE DISTRIBUTIONS IN 3-SAT

In this section, we establish the nomenclature of the 3-SAT problem as well as the concept of clause-types, and describe the mapping to an Ising Hamiltonian. We briefly discuss SLS algorithms exemplified by the WALKSAT heuristic, and then show how their performance is

intimately linked to the aforementioned statistics of the problem instances.

A. From combinatorics to Ising Hamiltonians

In combinatorial optimization, a 3-SAT problem consists of N Boolean *variables* $\mathbf{x} = (x_1, \dots, x_N)$. The x_n are constrained by $M = \alpha N$ clauses, with the *clause density* α . Each clause $C_m = l_{m_1} \vee l_{m_2} \vee l_{m_3}$ connects three *literals* via a logical or, where each literal l can represent either a variable x or its negation \bar{x} . A full 3-SAT problem is simply the conjunction of all clauses $C_1 \wedge \dots \wedge C_M$, referred to as conjunctive normal form (CNF), requiring that all clauses must be satisfied simultaneously.

In statistical physics, this problem may be equivalently represented as an Ising spin Hamiltonian

$$H = \sum_{m=1}^M \tilde{C}_m, \quad (1)$$

where the terms $\tilde{C}_m = P(l_{m_1})P(l_{m_2})P(l_{m_3})$ are defined with the projectors $P(l_n) = \frac{1 - \text{sgn}(l_n)\sigma_n}{2}$. Here, a negative sign of l_n corresponds to a negated variable \bar{x}_n . Physically we may think of $\sigma_n \in \{\pm 1\}$ as spins with $\sigma_n = 2x_n - 1$. Each clause has an *energy* E of zero if it is satisfied and an energy of one otherwise. For a state \mathbf{x} , the total energy is then simply defined as

$$E(\mathbf{x}) = \text{number of clauses violated by } \mathbf{x}, \quad (2)$$

such that a ground-state \mathbf{s} (or *solution*) must satisfy all clauses and therefore have $E(\mathbf{s}) = 0$. In the spin representation, the problem is equivalent to $H\boldsymbol{\sigma} = E\boldsymbol{\sigma}$, where solutions are zero-energy eigenvectors of H .

B. Clause type distribution space

On a more detailed note, each clause represents a constraint in the space of 2^N possible states, and e.g. $C_1 = \bar{x}_2 \vee x_4 \vee \bar{x}_5$ is satisfied by 7 out of the $2^3 = 8$ possible assignments to the involved triplet of variables. For one of these, say $x_2 = 0$, $x_4 = 0$ and $x_5 = 1$, the individual literals of the clause C_1 become either *true* ($\bar{x}_2 = 1$) or *false* ($x_4 = 0$, $\bar{x}_5 = 0$). We say that a clause is type- k if it has exactly k true literals, and we define

$$m_k(\mathbf{x}) = \text{number of type-}k \text{ clauses given } \mathbf{x}, \quad (3)$$

noting that $m_0 \equiv E$ is the number of unsatisfied clauses. We are usually more interested in the relative number of clause-types and therefore introduce the ratios

$$r_k(\mathbf{x}) = \frac{m_k(\mathbf{x})}{M} \in [0, 1]. \quad (4)$$

We refer to $\mathbf{r} = (r_0, \dots, r_3)$ as the clause-type distribution (CTD) of a state \mathbf{x} , which admits the normalization

$\sum_{k=0}^3 r_k(\mathbf{x}) = 1$, and we refer to the set of all possible \mathbf{r} as the clause-type distribution space (CTDS). Note that because a solution \mathbf{s} has $r_0 = 0$, i.e. no unsatisfied (type-0) clauses, the normalization implies that the two numbers $r_1(\mathbf{s})$ and $r_2(\mathbf{s})$ are sufficient to parameterize the solution-subspace of the full CTDS of 3-SAT.

C. Stochastic local search

Stochastic local search (SLS) solvers generally try to solve a satisfiability problem via a focused search starting from a random initial state \mathbf{x} , iteratively flipping the value of variables chosen by a heuristic [41–44]. Focused means that every iteration of the algorithm starts by (randomly) selecting one of the violated constraints (type-0 clauses), which has the benefit of satisfying the chosen clause regardless of which of its variables is selected. This process is iterated for a certain number of flips, after which the search is usually restarted from a new random state. The key ingredient of such SLS algorithms then lies in their heuristic selection process of variables and clauses.

With the *walk probability* p_{walk} , the well established SLS heuristic WALKSAT picks a random variable from a randomly chosen type-0 clause, while with $1 - p_{\text{walk}}$ it instead performs a greedy step by picking the variable with minimal breakcount b in that clause [41]. The breakcount b_n for a variable x_n is the number of clauses that would be broken by flipping x_n (i.e. the number of transitions from type-1 to type-0 clauses). For completeness, we note that WALKSAT always picks a variable with $b_n = 0$ if it exists in the selected clause (i.e. “free” moves are preferred), and that any ties are broken randomly.

D. Satisfiable random problems with fixed CTD

We now clarify where the hardest 3-SAT problems are expected to be found for a given problem size N . In *random uniform* instances, clauses are generated by choosing three variables out of the available N as literals, and to negate each of them independently with probability $\frac{1}{2}$. Finding solutions to such problems is comparably well under control. More specifically, they are known to undergo a phase transition at a critical clause density of $\alpha_c \approx 4.262$ [31], beyond which instances are unsatisfiable with high probability [12, 29, 30]. Below α_c , the solutions are well understood theoretically via the cavity method [32, 33] and also exploitable computationally via the SURVEY PROPAGATION (SP) algorithm derived from it [37, 38]. As α approaches the phase transition, the initially connected solution space shatters into exponentially many small clusters, which eventually vanish at α_c . We refer to such solutions as *accidental*, because they originate from a lack of constraints and always exist for sufficiently small $\alpha < \alpha_c$ unless there is additional struc-

ture in the problem that prevents their formation (e.g. finite interaction ranges).

Since SP can find these states even beyond $N = 10^5$, $\alpha < \alpha_c$ is clearly not “as hard as it gets” for 3-SAT and we therefore require $\alpha \gtrsim \alpha_c$. To ensure existence of zero-energy ground-states for larger α , modified (non-uniform) protocols for generating hard solvable instances have been introduced [39]. Such problems have a hidden solution at a predetermined CTD (i.e. fixed r_1 and r_2 ; cf. Appendix A), and a *critical* [40] parameter-line has been predicted for which finding the solution is hardest [39]. Here, we study more broadly how r_1 and r_2 affect the problem difficulty. To suppress the coexistence probability of usually easier to find accidental solutions, we consistently choose $\alpha > \alpha_c$ by a finite margin in the following. Specifically, to mitigate finite-size effects at moderate N , we set $\alpha = 5$ so as to avoid accidental solutions entirely for all studied system sizes. We note that the higher number of constraints may make the problems “slightly less hard” [52] for complete solvers such as CADICAL [47], but these differences are minor close enough to α_c . In this light, we emphasize that $\alpha = 5$ may make the performance comparison in Appendix B somewhat unfavorable for our SLS algorithm, but improves the clarity of the numerical results for finite N , and is thus a conservative choice for our subsequent benchmarks.

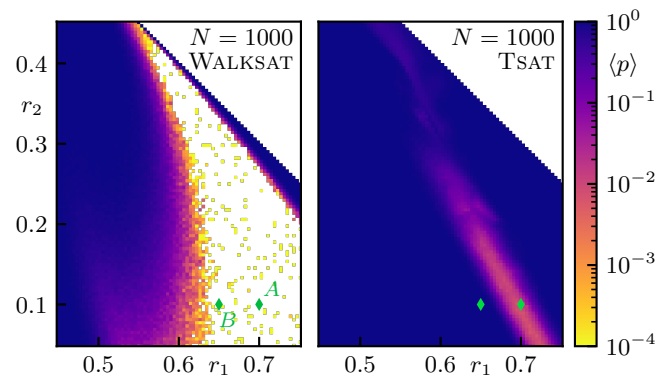


FIG. 2. Average success probability $\langle p \rangle$ of WALKSAT (left panel) and TSAT (right panel) for problems generated via Algorithm 2. At each point in CTDS we generate 10^2 instances with $N = 1000$ and $\alpha = 5$, using 10^2 trials per instance and $300N$ flips per trial (cf. Appendix C for solver specific parameters). Even on the clearly distinguished critical line $r_2 = \frac{3}{2} - 2r_1$ predicted to harbor the most difficult problems, TSAT still manages to solve most problems and maintains a comparably high success probability ($\geq 0.6\%$). For WALKSAT, we find two transitions to an extended intractable region which contains but is not limited to the critical line. Note that accidental solutions have $(r_1, r_2) \approx (0.46, 0.41)$, and thus belong to a region that is comparably easy. For the point $A = (0.7, 0.1)$ on and the point $B = (0.65, 0.1)$ below the critical line, we compare the dependence on N in Fig. 3.

The aforementioned critical line of hardest problems is predicted to be located at $r_2 = \frac{3}{2} - 2r_1$ for $r_3 \gtrsim 0.08$ [39]. The line coincides with the simple condition that half the

literals in the hidden solution should be true, and in the language of statistical physics this is equivalent to the statement that the local field (i.e. the terms linear in σ_n in the Hamiltonian) should be zero for all variables. The criterion about the starting point of the line at finite r_3 translates to the sudden onset of an extensive number of frozen variables in the solution (i.e. variables that take the same value in every solution) [39]. We will later see in Section V that this point corresponds to the location of a barrier in CTDS that takes exponential time to traverse. Fig. 2 shows the average success probability $\langle p \rangle$ of individual trials for WALKSAT and our TSAT on problems generated using Algorithm 2 throughout the CTDS at $N = 1000$ variables. We find that for WALKSAT, $\langle p \rangle$ strongly depends on the position in CTDS: There exist extensive regions in which none of the 10^2 problems could be solved within the 10^2 trials per instance, and the transitions between easy and hard regions are quite sharp. This indicates that the CTD of the hidden solution indeed significantly impacts computational hardness for established SLS algorithms, and that problems even relatively far away from the critical line can be intractable for them. TSAT on the other hand retains a comparably high success probability $\geq 0.6\%$ throughout CTDS, and the critical line is clearly distinguished as the location of the hardest problems. In Section IV, we discuss the scaling of $\langle p \rangle$ as a function of N for the two highlighted points $A = (0.7, 0.1)$ on the critical line and $B = (0.65, 0.1)$ slightly below it.

III. TARGETING CLAUSE-TYPE DISTRIBUTIONS

In this section, we develop a SLS heuristic coined TARGET-SAT (TSAT) that can guide the search toward a given target point in CTDS. Conceptually, specifying a target distribution amounts to selecting a sufficiently suitable picklock for the given problem instance out of (polynomially many) possible options. On a more technical level, aside from the unique scoring function we also introduce the option to select already satisfied clauses as a valuable resource for overcoming barriers.

A. Scoring via clause-type transitions

In order to navigate the CTDS, our TSAT heuristic keeps track of all *transitions* between type- k clauses caused by a potential variable flip. For 3-SAT, there are six possible transitions: $t_{k \rightarrow k+1}$ for $k = 0, 1, 2$ and $t_{k \rightarrow k-1}$ for $k = 1, 2, 3$ true literals. Note that the breakpoint relevant for WALKSAT corresponds to $b_n = t_{1 \rightarrow 0}(x_n)$. The change in the number of type- k clauses upon flipping variable x_n , which we formally define as

$$\Delta_k(x_n) = m_k(\mathbf{x} \text{ after flipping } x_n) - m_k(\mathbf{x}), \quad (5)$$

can be calculated from the transition counts via

$$\Delta_k = t_{k+1 \rightarrow k} - t_{k \rightarrow k+1} + t_{k-1 \rightarrow k} - t_{k \rightarrow k-1}, \quad (6)$$

where terms with invalid indices are neglected (affects $k = 0, 3$). Now suppose that the current CTD is $\mathbf{m}(\mathbf{x})$, and that the targeted CTD is \mathbf{t} . Then we define the distance vector $\mathbf{d} = \mathbf{t} - \mathbf{m}$, such that $d_0 = -m_0 = -E$, and introduce the scalar *distance-to-target* as

$$\Delta_{\text{CTDS}} = \|\mathbf{d}\|_1 = \sum_{k=0}^3 |t_k - m_k|. \quad (7)$$

We seek to minimize this distance, and thus define the *score* of variable x_n as

$$s_n = b_n + \sum_{k=1}^3 g_k |d_k - \Delta_k|. \quad (8)$$

Here, $\mathbf{g} = (g_1, g_2, g_3)$ is a vector of couplings constants (i.e. algorithm parameters). While one can certainly imagine different and also more complex scoring heuristics, Eq. 8 already incorporates two ideas: First, the score is proportional to the magnitude of the changes Δ_k . Second, by measuring the distance to d_k we ensure that we prefer a move that actually brings us closer to the target (i.e. this deals with cases of overshooting). One could consider introducing a dependence on d_k in the couplings g_k , but we will see in Section V that the bottleneck in the hardest problems lies in a highly localized barrier for which g_k would remain approximately constant anyway.

To pick one of the three variables in a clause, we compute each score and then use a standard Boltzmann distribution with inverse temperature β to select one, i.e. $P(x_n) \sim e^{-\beta s_n}$. Because $s_n \sim d_n \sim M$, it is helpful to subtract the average score $\langle s \rangle$ from s_n in the exponent to avoid numerical problems. This is also why the score is effectively proportional to Δ_k , as the d_k is the same for every s_n and thus cancels unless one is already very close to the target.

B. Selecting satisfied clauses

The scoring heuristic in Eq. 8 on its own can already significantly improve performance. However, because of substantial energy barriers en-route to the target CTD (cf. Fig. 1), we found that it can be very helpful to also assign a probability to select clauses that are already satisfied, but are of a type that we have too many of. As an illustrative example, consider that we are at $\mathbf{m} = (5, 25, 15, 5)$ but we want to reach $\mathbf{t} = (0, 35, 5, 10)$. Then the main obstruction is the abundance of type-2 clauses, which we can reduce by selecting one of them with a certain probability. To achieve this, we define the (unnormalized) probability to select a type- k clause as $p_k = -d_k$, truncating negative values to zero. For the above example this would give $p_0 = 5$ and $p_2 = 10$, but

it turns out that this is usually too skewed toward p_2 . To allow for some more control we scale the p_k by a sigmoid,

$$p_k \rightarrow p_k \cdot \frac{a_{\text{ampl}}}{1 + \exp\left[-a_{\text{sharpness}}\left(\frac{p_k}{p_0} - 1\right)\right]} \quad (9)$$

for $k = 1, 2, 3$. The precise shape of this transition is found to be of minor quantitative importance and we always set $a_{\text{sharpness}} = 4$ in the following, while the amplification $a_{\text{ampl}} \approx 0 \dots 2$ is found to have a much bigger impact, and is thus adjusted as a model parameter. For details on model parameters used in all benchmarked algorithms, see Appendix C. Finally, the probability to pick a type- k clause is given by $P_k = p_k / \sum_{k=0}^3 p_k$. The full variable selection process in TSAT is summarized in Algorithm 1.

Algorithm 1 Variable selection in TSAT

Require: target t_k , and tables for Δ_k and m_k (Eq. 5 and 6)

- 1: compute p_k using Eq. 9 and normalize to P_k
 - 2: $k \leftarrow$ random value based on probabilities (P_0, \dots, P_3)
 - 3: clause \leftarrow random type- k clause
 - 4: compute the scores for variables in clause using Eq. 8
 - 5: $x_n \leftarrow$ random variable with probability $\sim e^{-\beta s_n}$
 - 6: **return** x_n
-

Note that giving away the CTDS target information merely reduces the exponentially large search space by a polynomial amount since one could simply try out all the $\sim N^2$ possible target options (although more sophisticated search strategies are of course also conceivable).

IV. PERFORMANCE BENCHMARKS

In this section, we zoom in on the system size scaling for the two points in CTDS highlighted in Fig. 2 to illustrate how the problem difficulty changes depending on the underlying target distribution. We also compare the performance to WALKSAT and our recent DOCSAT [51].

For the point $A = (0.7, 0.1)$ right on the critical line, which includes the most difficult known solvable problems, Fig. 3(a) shows that TSAT roughly triples the average accessible system size, which is remarkable given the exponential hardness of the problem. The initially sub-exponential decay in the success probability $\langle p \rangle$ (implying sub-exponential runtime $\sim 1/\langle p \rangle$) eventually transitions to the expected exponential decay around $N \approx 500$. At this system size, many problem instances are already intractable for other algorithms (including powerful complete solvers, cf. Appendix B). While these problems are therefore evidently hard, they now look qualitatively easier thanks to the softer scaling of TSAT at these values of N . Also note that the performance of e.g. WALKSAT is much more instance dependent, leading to a substantially larger variance: In particular, the first unsolved instances in this dataset are already at a mere $N = 100$ ($N = 200$) variables for WALKSAT (DOCSAT), while only at $N = 1000$ for TSAT.

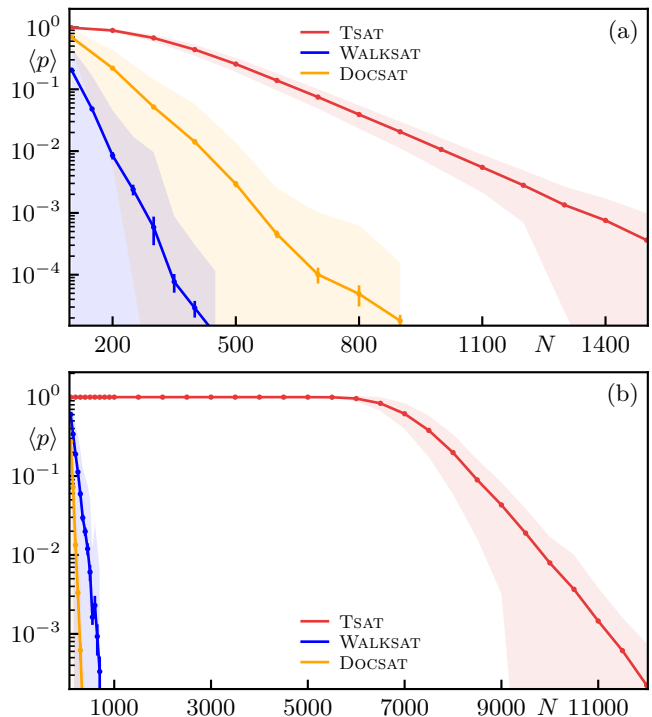


FIG. 3. (a) Average success probability $\langle p \rangle$ of an individual trial for WALKSAT, DOCSAT and TSAT for $A = (0.7, 0.1)$ (10^3 instances at each N and 10^3 trials). Consistent with the ratio of solved instances, TSAT shows the softest exponential decay and almost triples the accessible system size (runtime is $\sim 1/\langle p \rangle$). Also note that the variance is much smaller for TSAT, i.e. its performance is less instance dependent (shaded region marks the standard deviation). (b) At $B = (0.65, 0.1)$, i.e. slightly below the critical line, the performance advantage of TSAT is even more striking. Interestingly, TSAT shows a rather sudden transition toward exponential scaling around $N \approx 6000$, which we investigate in Section V.

For the point $B = (0.65, 0.1)$ slightly below the critical line the success probability shown in Fig. 3(b) is again exponential for WALKSAT and DOCSAT, but here the latter performs significantly worse (cf. Appendix B). TSAT meanwhile shows a very interesting transition from an apparently trivial to an exponentially hard regime around $N \approx 6000$, which is an order of magnitude beyond problem sizes accessible via other methods. To understand this rather sudden change in scaling we have to take a closer look at the typical TSAT search trajectories through CTDS, which we analyze next.

V. DISTINGUISHING TWO TYPES OF COMPLEXITY BARRIERS

In this section, we discuss in more detail the TSAT trajectories through CTDS as illustrated in Fig. 1. In summary, we find that the difficulty of the full problem is captured by two different types of complexity barriers.

ers, both of which are prominently featured in Fig. 1. One of these encompasses the *final search* phase at very low energy in the vicinity of the targeted CTD, and its size only shows a moderate dependence on the location of the hidden solution. Since the neighborhood of this CTD is an extensive subset of the full search space, it still contains exponentially many states, and therefore leads to a relatively soft but quite generic exponential wall, reflecting the NP-complete nature of the problem. Interestingly, we also find that there exists a second barrier that strongly depends on the position in CTDS and represents a different kind of complexity. It can dwarf the final search barrier by orders of magnitude in certain regions including the critical line, which allows us to elucidate why WALKSAT and other SLS algorithms have such a difficulty solving those problems. To elaborate on the behavior of this additional barrier, in the following we analyze two representative points in CTDS, marked as A and B in Fig. 2.

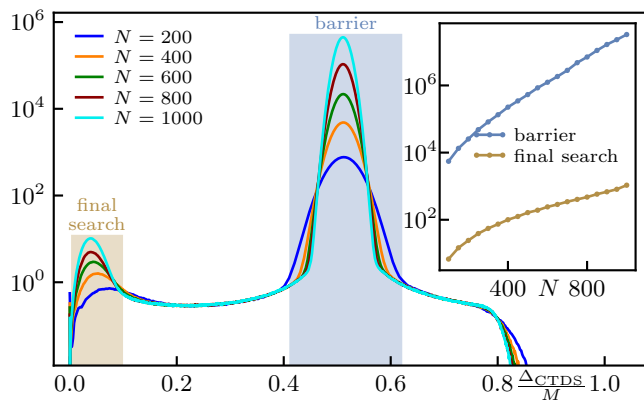


FIG. 4. For varying size N , we run TSAT on 10^2 instances at $A = (0.7, 0.1)$ for 10^2 trials each, with unlimited flips per trial (until a solution is found). The plot shows a histogram of the number of states \mathbf{x} found at a certain distance-to-target (cf. Eq. 7), with random initial states situated on the right and solutions near $\Delta_{\text{CTDS}} \approx 0$ on the left. With increasing N , two peaks emerge and the search is dominated by the time it takes to traverse the barrier at $\Delta_{\text{CTDS}}/M \approx 0.5$. Outside the shaded regions marking the peaks all lines coalesce, indicating that navigating the CTDS takes $\mathcal{O}(N)$ time in those regions. The inset shows the total number of states in the two peaks as a function of N . Both the barrier and final search time remain sub-exponential up to surprisingly large N before transitioning to exponential scaling, which mirrors the success probability of TSAT in Fig. 3(a).

A. Complexity barriers on the critical line

First, consider the point $A = (0.7, 0.1)$ on the critical line, in the vicinity of which problems are particularly difficult. There, as shown in Fig. 4, the solution time is dominated by two diverging timescales: As already discussed, the final search phase is expected to take ex-

ponentially long. However, on the critical line a second timescale emerges due to a narrow but extensive barrier in CTDS around $\Delta_{\text{CTDS}}/M \approx 0.5$. This additional *barrier time* is not only exponential, but also increases much faster than the timescale of the final search (cf. Fig. 4 inset), such that the runtime is dominated by the time it takes TSAT to reach the target region in CTDS. This insight also explains more deeply why WALKSAT and other algorithms struggle so much with these problems, as they not only search in a part of the CTDS that does not contain the solution, but that is even separated from it by a large barrier rendering accidental success exceedingly improbable.

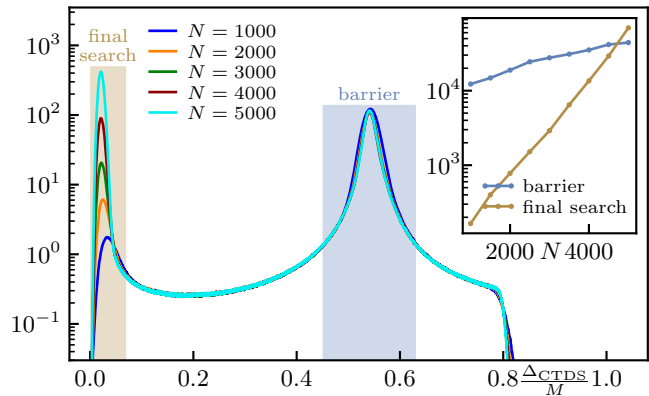


FIG. 5. Setup as in Fig. 4, but at $B = (0.65, 0.1)$. Away from the critical line the initial barrier appears to increase only linearly (note that the number of bins along the x -axis is $\propto N$, hence the coalescence of all lines). This explains why TSAT retains an average $\langle p \rangle \approx 1$ in Fig. 3(b) up to very large N ; beyond $N \approx 5000$ the final search phase becomes the bottleneck (see crossing in the inset), and thus eventually inhibits solubility.

Another interesting observation in Fig. 4 is the coalescence of all system sizes in the regions away from the two barrier peaks. Because Δ_{CTDS} is discrete and $\sim M$, the number of bins in the histogram is linear in N (thus the integrated number of states is roughly \propto peak height $\times N$). That all curves coalesce between distances of about 0.1 to 0.4 (similarly 0.65 to 0.8) implies that it takes TSAT a linear number of steps to reach the final search region before and after traversing the main barrier. Thus, each individual step in CTDS toward the target in these regions actually takes only a constant time $\mathcal{O}(1)$ independent of system size. Put differently, navigating the CTDS appears to rapidly transition from exponentially hard to negligible.

B. Complexity off the critical line

Moving slightly away from the critical line to the point $B = (0.65, 0.1)$, the runtime is now asymptotically dominated by the final search, because the barrier scales linearly (at least for the accessible system sizes). However,

although the final search eventually becomes the bottleneck, the break-even size is only around $N \approx 5000$, and thus completely out of reach of any other algorithm (cf. Fig. 5). We again stress that the x -axis has $\propto N$ many steps, which is why the barrier time in the inset still increases linearly despite the coalescing lines.

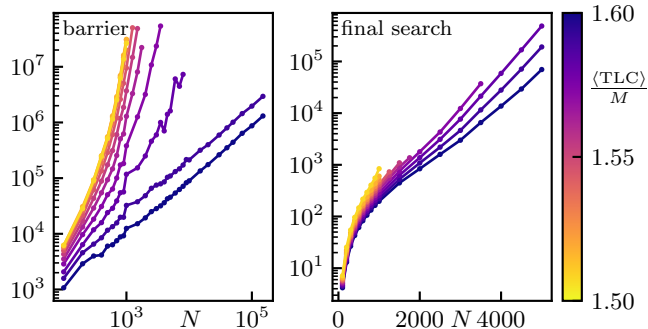


FIG. 6. Total number of states in the barrier (left panel) and final search phase (right panel) as a function of system size N for various equidistant average TLC per clause of the hidden solution. The starting point is $B = (0.65, 0.1)$ at $\langle \text{TLC} \rangle / M = 1.6$ true literals per clause (cf. Fig. 5) and decreasing the TLC moves perpendicularly toward the critical line situated at $\langle \text{TLC} \rangle / M = 1.5$. The final search always becomes exponentially expensive and in particular shows only a mild dependence on the position in CTDS. Sufficiently far away from the critical line the barrier appears to remain linear for all explored system sizes. Close to the line, the barrier dwarfs the final search by orders of magnitude for a given N (see also Fig. 4).

Finally, in Fig. 6 we study how the scaling of the barrier and final search phase change as a function of distance from the critical line. The deviation perpendicular to the critical line is encoded in the average number of true literals per clause,

$$\frac{\langle \text{TLC} \rangle}{M} = 0 \cdot r_0 + 1 \cdot r_1 + 2 \cdot r_2 + 3 \cdot r_3, \quad (10)$$

where the true literal count (TLC) is the total number of true literals in a given state [51]. At the point $B = (0.65, 0.1)$ we have $\langle \text{TLC} \rangle / M = 1.6$, where, as in Fig. 5, the final search asymptotically dominates the sub-exponential barrier. As one approaches the point $(0.69, 0.12)$ on the critical line with $\langle \text{TLC} \rangle / M = 1.5$, the barrier regains its sharp exponential scaling while the final search only shows a mild increase. Note that the instance-to-instance variance of the barrier time appears to significantly increase around $\langle \text{TLC} \rangle / M \approx 1.58$ (cf. third line from the bottom in Fig. 6). This behavior may hallmark a criticality separating the exponential barrier from linear scaling. As to what extent the parameter regime exhibiting exponential scaling may be further narrowed toward the critical line (or even overcome) by further algorithmic improvements remains an intriguing question for future work.

In the linear barrier regime, we note that we can abort the TSAT trials once the barrier is passed, making it possible to check the linear scaling well beyond $N = 10^5$ without having to actually solve the problems (which would be prohibitively difficult due to the exponential final search). Finally, we note that on the other side of the critical line, toward $\langle \text{TLC} \rangle / M = 1.4$, the overall situation is qualitatively similar as discussed above.

VI. CONCLUDING DISCUSSION

We have shown how targeting a specific clause type distribution can efficiently guide stochastic local search toward a hidden solution, thus unlocking a vast range of random satisfiability problems, including a significant advance of the tractable systems sizes in the hardest known parameter regime. This approach reveals and establishes CTDS as a natural phase space for solvable random 3-SAT instances beyond the comparably manageable random uniform problems. The resulting TSAT algorithm largely improves on and generalizes our previous heuristic DOCSAT [51] which in hindsight may be seen as targeting a lower dimensional cut through the full CTDS by simply reducing oversatisfied constraints (clauses with more than one true literal).

Besides the mere improvement in performance, our analysis also provides deep insights into the specific complexity of random 3-SAT instances in stochastic local search. In particular, apart from isolated points in the explored CTDS, all instances, whether on the critical parameter line or not, exhibit a final search barrier in the vicinity to the solution that scales exponentially in problem size. This highlights the generic exponential complexity of solving random 3-SAT problems in agreement with the exponential time hypothesis [13]. Interestingly, the critical parameter line in CTDS is distinguished by an additional barrier far away from the solution that dominates the local search and represents the clear bottleneck for the tractable system sizes. By contrast, away from the critical parameter line TSAT quickly overcomes this additional barrier in sub-exponential time, hence rendering the aforementioned final search the limiting structure, and explaining the rapid increase in solvable system sizes.

On a broader note, in this work we have made significant progress on solving hard random 3-SAT instances, and the principle of TSAT may readily be generalized to higher-dimensional CTDS so as to tackle k -SAT with $k > 3$ as well as more generalized satisfiability problems with mixed clause lengths. This being said, we would like to emphasize some key limitations and remaining open problems. First, for instances that are not guaranteed to have a solution, proving their unsatisfiability remains a hard task for which complete solvers such as CADICAL are leading. Second, while the considered random problems are certainly most interesting in statistical physics and computational complexity theory, it remains to be seen as to what extent the principle behind TSAT

may also lead to synergies in solving highly structured (or practical) problems. There, the main challenge is to efficiently exploit a given non-generic structure to solve much larger system sizes (often $N \sim 10^6$), where the lead has so far also remained firmly in the realm of complete solvers.

ACKNOWLEDGMENTS

We acknowledge discussions with Tim Pokart and Yumin Hu as well as financial support from the German Research Foundation (DFG) through the Collaborative Research Centre (SFB 1143, project ID 247310070) and the Cluster of Excellence ctd.qmat (EXC 2147, project ID 390858490).

Appendix A: Generating problems at fixed CTD

In order to generate random but satisfiable 3-SAT problem instances at a fixed position in CTDS we use the ideas from [39]. Assuming that $\mathbf{x} = (1, \dots, 1)$ is our hidden solution, we generate the requested number of $m_k = Mr_k$ type- k clauses by choosing k variables and $3 - k$ negated variables as literals ($k = 1, 2, 3$). Finally, the solution is scrambled by negating each literal associated with a variable x_n with probability $\frac{1}{2}$ for each $n = 1, \dots, N$ (cf. Algorithm 2).

Algorithm 2 Satisfiable random 3-SAT at fixed CTD

Require: N variables, M clauses and r_1, r_2

- 1: CNF \leftarrow empty list of clauses
- 2: **for** $k = 1, 2, 3$ **do** \triangleright type- k clauses
- 3: $m_k \leftarrow Mr_k$ $\triangleright m_3 = M - m_1 - m_2$
- 4: **for** $m = 1, \dots, m_k$ **do**
- 5: clause \leftarrow 3 random variables from $\{x_1, \dots, x_N\}$
- 6: randomly negate $(3 - k)$ of the literals in clause
- 7: add clause to CNF
- 8: **end for**
- 9: **end for**
- 10: **for** $n = 1, \dots, N$ **do** \triangleright scramble the hidden solution
- 11: **if** $\text{RANDOMUNIFORM}(0, 1) < \frac{1}{2}$ **then**
- 12: swap every occurrence of x_n and \bar{x}_n in CNF
- 13: **end if**
- 14: **end for**
- 15: **return** CNF

Appendix B: Comparison to other solvers

Here, we compare TSAT’s performance to established algorithms, namely the very powerful complete solver CADICAL [47, 53] based on conflict-driven clause learning, the SLS algorithm YALSAT [54], and the message passing algorithm SP [37, 38]. In Fig. 7, we show the ratio of solved problems R_{sol} as a function of N for (a) the point $A = (0.7, 0.1)$ on the critical line and (b) the point $B = (0.65, 0.1)$ slightly below it (cf. Fig. 3). For

both points, SP only manages to fix at most a handful of spins before reporting a paramagnetic state, at which stage the reduced problem is passed to WALKSAT. Hence, the performance is almost identical to WALKSAT due to using the same number of total flips for both methods. The performance of CADICAL is mostly unaffected by the CTD of the hidden solution, and the algorithm overall benefits slightly from the increased conflict-rate due to $\alpha > \alpha_c$. However, due to the lack of structure in these random problems, it is still limited to $N \lesssim 500$. Even for these hardest problems TSAT almost triples the accessible system size, while the advantage is well beyond an order of magnitude at the point B . Our recent DOCSAT heuristic [51] performs well at A , even solving some problems beyond CADICAL, but works poorly at B , which we discuss next.

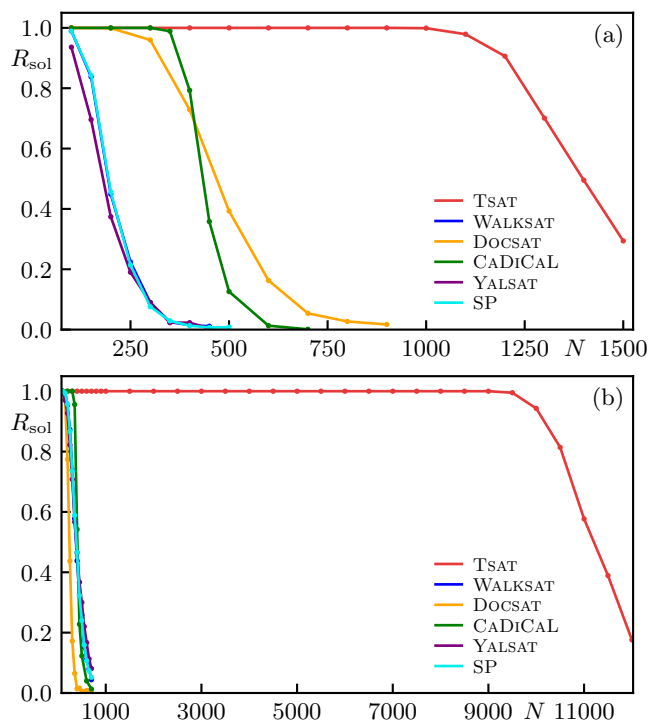


FIG. 7. Ratio R_{sol} of solved instances for 10^3 problems and various algorithms (cf. Appendix C for parameters). (a) At the point $A = (0.7, 0.1)$ on the critical line in CTDS, WALKSAT, YALSAT and SP do not perform well, but the complete solver CADICAL benefits from the increased conflict-rate due to the larger than critical $\alpha = 5$. DOCSAT still scales slightly better, while TSAT triples the accessible system size. (b) At the point $B = (0.65, 0.1)$, DOCSAT performs poorly below the critical line (cf. Fig. 8). The other four algorithms are more similar, while TSAT stands out by solving all problems up to $N = 10^4$.

DOCSAT is based on a direct modification of WALKSAT with the purpose of guiding toward a desired global true literal count (TSAT draws inspiration from and generalizes this concept). The concrete implementation of DOCSAT slightly favors variable flips that reduce the total

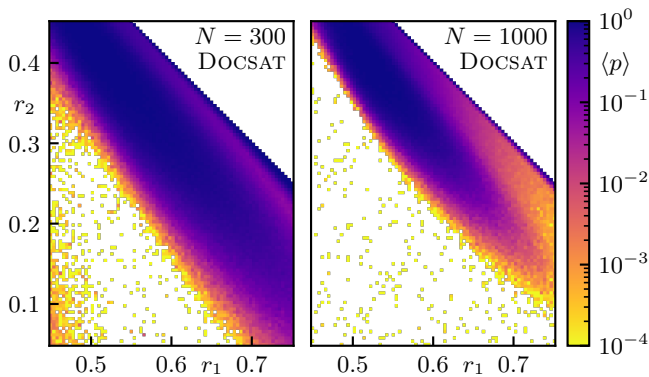


FIG. 8. Average success probability $\langle p \rangle$ of DOCSAT for problems at various points in CTDS (cf. Fig. 2). The ratio of true literals in the hidden solution is $1 - \frac{2r_1+r_2}{3}$, while DOCSAT empirically operates near a ratio of ≈ 0.53 (as opposed to ≈ 0.55 for WALKSAT). This explains the poor performance below the critical line, but also why DOCSAT significantly outperforms WALKSAT in some regions.

number of true literals in the problem, essentially moving perpendicular to the critical line in CTDS. On average, the ratio of true literals for WALKSAT is ≈ 0.55 (which agrees well with the ratio for accidental solutions), while DOCSAT operates at a lower value of ≈ 0.53 . Even though this may appear to be a small change, the effect on the performance throughout CTDS is dramatic as illustrated in Fig. 8: DOCSAT manages to improve drastically on WALKSAT in a part of the CTDS, in particular around the parameters studied in [51], while failing to solve most problems below the critical line (which includes the point B). This is because the ratio of true literals in the hidden solution is $1 - \frac{2r_1+r_2}{3}$, which is $\frac{1}{2}$ on the critical line and larger than $\frac{1}{2}$ below it, such that the lower ratio targeted by DOCSAT is only superior to WALKSAT for problems situated close to or above the line. When compared with Fig. 2, one may view DOCSAT as quite complementary to WALKSAT in CTDS. Importantly, the strong regime of DOCSAT contains the critical parameter line, even though the advantage to other solvers there decreases with increasing r_1 (decreasing r_2).

Appendix C: Algorithm Parameters

WALKSAT: We set $p_{\text{walk}} = 0.5$ and note that different values have a marginal impact on the results, as was also the case in our previous study [51]. Unless noted otherwise, we run 10^3 trials on every problem instance with a cutoff of $300N$ flips per trial.

DOCSAT: As in [51], we set $p_{\text{walk}} = 0.4$ and $r_{\text{doc}} = 0.15$. Flips and trials as for WALKSAT.

TSAT: We have optimized the parameters β , a_{ampl} and g for individual points from the CTDS, interpolating inbetween. While these parameters yield substantially better results than a fixed global set, no fine-tuning is required in the sense that say $g_2 = 0.2$ is not much different from $g_2 = 0.1 \dots 0.3$, while $g_2 = 0$ or $g_2 = 1$ may lead to significantly worse performance. Flips and trials as for WALKSAT.

SP: We fix 1% of variables per loop of the SP-iteration, with a limit of 10^3 steps (that is rarely exhausted) and an error tolerance of $\epsilon = 10^{-3}$ (same parameters as in [37]). We use 25 full restarts of the SP elimination procedure with 40 WALKSAT trials after each (matching the total number of 10^3 trials). Because variables may be fixed to the wrong value (i.e. rendering an instance unsatisfiable), SP can perform worse than pure WALKSAT in some cases despite the increased runtime. For problems near the critical line, performance is almost identical to WALKSAT because very few variables are fixed by SP.

YALSAT: Fewer full restarts appear to perform better for this algorithm, so we use 10^2 trials with $3000N$ flips each. Other parameters as in the default configuration.

CADICAL: We have configured the solver to target satisfiable instances, which to our knowledge mainly impacts the restart interval. The runtime scales slightly superlinear in the number of decisions, and a limit of $3000N$ yields runtime comparable to the other algorithms (but favoring CADICAL).

-
- [1] F. Barahona, *Journal of Physics A: Mathematical and General* **15**, 3241 (1982).
- [2] A. Lucas, *Frontiers in Physics* **2**, 5 (2014).
- [3] G. Parisi, *Phys. Rev. Lett.* **43**, 1754 (1979).
- [4] G. Parisi, *Journal of Physics A: Mathematical and General* **13**, L115 (1980).
- [5] S. Boettcher and A. G. Percus, *Phys. Rev. Lett.* **86**, 5211 (2001).
- [6] L. Bieche, J. P. Uhry, R. Maynard, and R. Rammal, *Journal of Physics A: Mathematical and General* **13**, 2553 (1980).
- [7] C. K. Thomas and A. A. Middleton, *Phys. Rev. B* **76**, 220406 (2007).
- [8] A. Hartmann and H. Rieger, *New Optimization Algorithms in Physics* (Wiley, 2006).
- [9] S. A. Cook, in *Proceedings of the Third Annual ACM Symposium on Theory of Computing*, STOC '71, edited by M. A. Harrison, R. B. Banerji, and J. D. Ullman (Association for Computing Machinery, New York, USA, 1971) p. 151–158.
- [10] R. M. Karp, Reducibility among combinatorial problems, in *Proceedings of a symposium on the Complexity of Computer Computations*, edited by R. E. Miller, J. W. Thatcher, and J. D. Bohlinger (Springer US, Boston, MA, 1972) pp. 85–103.

- [11] M. R. Garey and D. S. Johnson, *Computers and Intractability; A Guide to the Theory of NP-Completeness* (W. H. Freeman & Co., USA, 1990).
- [12] D. Achlioptas and C. Moore, *SIAM Journal on Computing* **36**, 740 (2006).
- [13] R. Impagliazzo and R. Paturi, *Journal of Computer and System Sciences* **62**, 367 (2001).
- [14] D. Dobrynin, A. Renaudineau, M. Hizzani, D. Strukov, M. Mohseni, and J. P. Strachan, *Phys. Rev. E* **110**, 045308 (2024).
- [15] O. Kullmann, Present and future of practical sat solving, in *Complexity of Constraints: An Overview of Current Research Themes*, edited by N. Creignou, P. G. Kolaitis, and H. Vollmer (Springer Berlin Heidelberg, Berlin, Heidelberg, 2008) pp. 283–319.
- [16] G.-J. Nam, K. A. Sakallah, and R. A. Rutenbar, in *International ACM Symposium on Field-Programmable Gate Arrays*, edited by S. Kaptanoglu and S. Trimberger (IEEE Computer Society, Los Alamitos, CA, USA, 1999) pp. 167–175.
- [17] S. Mukherjee and S. Roy, *Microelectronics Journal* **46**, 706 (2015).
- [18] J. Marques-Silva, M. Janota, and A. Belov, in *Proceedings of the 25th International Conference on Computer Aided Verification - Volume 8044, CAV 2013*, edited by N. Sharygina and H. Veith (Springer-Verlag, Berlin, Heidelberg, 2013) p. 592–607.
- [19] J. D. Park, in *Eighteenth National Conference on Artificial Intelligence* (American Association for Artificial Intelligence, USA, 2002) p. 682–687.
- [20] R. Dechter, *Constraint Processing* (Morgan Kaufmann, 2003).
- [21] Z. Xing and W. Zhang, *Artificial Intelligence* **164**, 47 (2005).
- [22] N. Ollikainen, E. Sentovich, C. Coelho, A. Kuehlmann, and T. Kortemme, in *2009 IEEE/ACM International Conference on Computer-Aided Design - Digest of Technical Papers* (2009) pp. 128–135.
- [23] D. Allouche, I. André, S. Barbe, J. Davies, S. de Givry, G. Katsirelos, B. O’Sullivan, S. Prestwich, T. Schiex, and S. Traoré, *Artificial Intelligence* **212**, 59 (2014).
- [24] A. Gupta, M. K. Ganai, and C. Wang, in *Formal Methods for Hardware Verification*, edited by M. Bernardo and A. Cimatti (Springer Berlin Heidelberg, Berlin, Heidelberg, 2006) pp. 108–143.
- [25] M. R. Prasad, A. Biere, and A. Gupta, *International Journal on Software Tools for Technology Transfer* **7**, 156 (2005).
- [26] G. P. Matos, L. M. Albino, R. L. Saldanha, and E. M. Morgado, *Public Transport* **13**, 625 (2021).
- [27] P.-H. Yuh, C. C.-Y. Lin, T.-W. Huang, T.-Y. Ho, C.-L. Yang, and Y.-W. Chang, in *International Workshop on System Level Interconnect Prediction* (2011) pp. 1–7.
- [28] D. V. Zhukov, D. A. Zheleznikov, and M. A. Zapletina, in *2020 IEEE Conference of Russian Young Researchers in Electrical and Electronic Engineering (EIconRus)*, edited by S. Shaposhnikov (2020) pp. 1905–1910.
- [29] P. Cheeseman, B. Kanefsky, and W. M. Taylor, in *Proceedings of the 12th International Joint Conference on Artificial Intelligence - Volume 1, IJCAI’91*, edited by J. Mylopoulos and R. Reiter (Morgan Kaufmann Publishers Inc., San Francisco, CA, USA, 1991) p. 331–337.
- [30] D. Mitchell, B. Selman, and H. Levesque, in *Proceedings of the Tenth National Conference on Artificial Intelligence*, AAAI’92, edited by P. Rosenbloom and P. Szolovits (AAAI Press, 1992) p. 459–465.
- [31] P. H. Lundow and K. Markström, *Phys. Rev. E* **99**, 022106 (2019).
- [32] S. Mertens, M. Mézard, and R. Zecchina, *Random Struct. Algorithms* **28**, 340–373 (2006).
- [33] M. Mézard, G. Parisi, and R. Zecchina, *Science* **297**, 812 (2002).
- [34] A. Coja-Oghlan, *J. ACM* **63**, 10.1145/3005398 (2017).
- [35] A. Coja-Oghlan, F. Krzakala, W. Perkins, and L. Zdeborova, in *Proceedings of the 49th Annual ACM SIGACT Symposium on Theory of Computing, STOC 2017*, edited by H. Hatami, P. McKenzie, and V. King (Association for Computing Machinery, New York, NY, USA, 2017) p. 146–157.
- [36] S. Hetterich, in *43rd International Colloquium on Automata, Languages, and Programming (ICALP 2016)*, Vol. 55, edited by I. Chatzigiannakis, M. Mitzenmacher, Y. Rabani, and D. Sangiorgi (Schloss Dagstuhl, 2016) pp. 65:1–65:12.
- [37] A. Braunstein, M. Mézard, and R. Zecchina, *Random Struct. Algorithms* **27**, 201–226 (2005).
- [38] R. Marino, G. Parisi, and F. Ricci-Tersenghi, *Nature Communications* **7**, 12996 (2016).
- [39] W. Barthel, A. K. Hartmann, M. Leone, F. Ricci-Tersenghi, M. Weigt, and R. Zecchina, *Phys. Rev. Lett.* **88**, 188701 (2002).
- [40] To clarify, the word critical here refers to the critically hard region within the parameter regime of the hidden solution at some fixed clause density α , and not to the critical value α_c that marks the phase transition toward unsatisfiability in random 3-SAT problems.
- [41] B. Selman, H. A. Kautz, and B. Cohen, in *Proceedings of the Twelfth National Conference on Artificial Intelligence (Vol. 1), AAAI ’94*, edited by B. Hayes-Roth and R. Korf (American Association for Artificial Intelligence, USA, 1994) p. 337–343.
- [42] H. H. Hoos and T. Stützle, *Journal of Automated Reasoning* **24**, 421 (2000).
- [43] H. H. Hoos and T. Stützle, Stochastic local search algorithms: An overview, in *Springer Handbook of Computational Intelligence*, edited by J. Kacprzyk and W. Pedrycz (Springer Berlin Heidelberg, Berlin, Heidelberg, 2015) pp. 1085–1105.
- [44] H. Fu, Y. Xu, S. Chen, and J. Liu, *JUCS - Journal of Universal Computer Science* **26**, 220 (2020).
- [45] J. Marques-Silva, I. Lynce, and S. Malik, Conflict-driven clause learning sat solvers, in *Handbook of Satisfiability*, *Frontiers in Artificial Intelligence and Applications* No. 1, edited by A. Biere, M. Heule, H. van Maaren, and T. Walsh (IOS Press, Netherlands, 2009) pp. 131–153, 1st ed.
- [46] N. Eén and A. Biere, in *Theory and Applications of Satisfiability Testing*, edited by F. Bacchus and T. Walsh (Springer Berlin Heidelberg, Berlin, Heidelberg, 2005) pp. 61–75.
- [47] A. Biere, T. Faller, K. Fazekas, M. Fleury, N. Froylyks, and F. Pollitt, in *Computer Aided Verification*, edited by A. Gurfinkel and V. Ganesh (Springer Nature Switzerland, Cham, 2024) pp. 133–152.
- [48] A. Biere, M. Heule, H. van Maaren, and T. Walsh, eds., *Handbook of Satisfiability*, *Frontiers in Artificial Intelligence and Applications*, Vol. 185 (IOS Press, 2009).

- [49] S. Alouneh, S. Abed, M. H. Al Shayeji, and R. Mesleh, *Artif. Intell. Rev.* **52**, 2575–2601 (2019).
- [50] J. K. Fichte, D. L. Berre, M. Hecher, and S. Szeider, *Commun. ACM* **66**, 64–72 (2023).
- [51] J. Schwardt and J. C. Budich, *Proceedings of the National Academy of Sciences* **122**, e2517297122 (2025).
- [52] C. Coarfa, D. Demopoulos, A. San Miguel Aguirre, D. Subramanian, and M. Vardi, Random 3-sat: The plot thickens, in *Principles and Practice of Constraint Programming*, Vol. 8, edited by R. Dechter (Springer Berlin, 2000) pp. 143–159.
- [53] A. Biere, T. Faller, K. Fazekas, M. Fleury, N. Frolenkovs, and F. Pollitt, in *Proc. of SAT Competition 2024 – Solver, Benchmark and Proof Checker Descriptions*, Vol. B-2024-1, edited by M. Heule, M. Iser, M. Jarvisalo, and M. Suda (University of Helsinki, 2024) pp. 8–10.
- [54] A. Biere, in *Proceedings of SAT Competition 2017 – Solver and Benchmark Descriptions*, Vol. B-1, edited by T. Tomáš, M. Heule, and M. Jarvisalo (University of Helsinki, 2017) pp. 14–15.